Inducing Crystallization of Polymer through Stretched Network

Baijin Zhao, Xiangyang Li, Youju Huang, Yuanhua Cong, Zhe Ma, Chunguang Shao, Haining An, Tinzi Yan, and Liangbin Li*

National Synchrotron Radiation Laboratory and Department of Polymer Science and Engineering, University of Science and Technology of China, Hefei, China

Received November 29, 2008
Revised Manuscript Received February 6, 2009

Introduction. Flow-induced crystallization of polymers is not only a fundamental nonequilibrium thermodynamic problem but also of importance for polymer processing and the final properties of polymer products. During polymer processing, such as extrusion, injection molding, and fiber spinning, polymer materials are subjected to various flow fields. Flow can enhance the crystallization rate up to several orders of magnitude and induce the formation of the so-called row nuclei or shish-kebab structure, which significantly increases the stiffness and thermo deformation temperature.[1−10] Although the benefit from flow field is widely recognized in academia and polymer industry, no satisfactory molecular theory has been achieved yet.

To explain flow-induced crystallization of polymer, entanglement−disentanglement (EDT) and coil−stretch (CS) transitions have been the basic ideas dominated in the community date back to Keller[11] and de Gennes.[12] They suggested that the flow-induced shish-kebab structure composes of extended long chains as row nuclei or shish and folded-chain crystals as kebab. Some recent elegant experiments and computer simulations further support the nucleation role of the oriented long chains.[13−17] However, a different picture presented by Kimata et al.[18] shows that the short chains or medium chains are more involved in the formation of shish. Indeed, more experimental evidence does not fit in the initial shish-kebab mechanism. Hsiao et al.[15] observed that a single lamella can grow from multiple shish instead of a single shish. Zhang et al.[19] showed that it is possible to produce row nuclei with a small shear rate and suggested EDT may not be a necessary condition for the formation of row nuclei. Without EDT, the stretched transient network is sufficient to accelerate crystallization and induce shish-kebab structure. With evidence from different facets, the two essential questions still remain as open debates, which prevent from further pursuing the molecular mechanism of the flow-induced crystallization of polymer. (i) What is the role of long and short chains in the formation of row nuclei or shish (or oriented nuclei in general)? (ii) What is the role of EDT in the formation of the oriented nuclei? We use "oriented nuclei" to emphasize on the enhancement of flow on nucleation in this work, as different structures such as point precursor, row nuclei, or shish-kebab can be produced by flow.

In this Communication, two simplified mixtures containing short free chains and chemically end-linked network were designed to answer the above-mentioned two questions, which resemble the transient network of polymer blend with short and long chains.[13−15,18] A schematic picture is illustrated in Figure 4A. These systems minimize the interferences of relaxation and macroscopic inhomogeneous of flow field, which may complicate the interpretation on the observed experimental phenomenon.[20,21] Similar systems had been employed to verify the initial reptation theory and other mechanism related to polymer dynamics.[21,22] Low molecular weight poly(ethylene oxide) (PEO) with a molecular weight of 2000 g/mol ($PEO2_F$) which has two acetyl end groups was used as the free chains. To build the end-linked network, the mesh size with molecular weights M of 2000 and 6000 g/mol, denoted as $PEO2_N$ and $PEO6_N$, were chemically cross-linked with 1,3,5-benzenetricarbonyl trichloride, respectively. As the critical entanglement molecular weight M_e of PEO is about 2000 g/mol,[23] and the chemical cross-linking points in network were considered as the permanent entanglements points, $PEO2_N$ resembles the high molecular weight PEO with permanent "entanglements", while $PEO6_N$ represents a polymer melt with about two possible disentanglement points.

Experimental Section. *Materials.* Two low molecular weight PEO fractions ($HO(CH_2CH_2O)_nH$) with weight-average molecular weight M_w = 2000 and 6000 g/mol, respectively, were purchased from Sinopharm Chemical Reagent Co. These PEOs possess two hydroxyl end groups. The coupling agent of 1,3,5-benzenetricarbonyl trichloride was purchased from Alfa Aesar. The PEOs (M_w = 2000 or 6000 g/mol) were dried under vacuum at 45 °C for 2 days before use.

$PEO2_F$ with two acetyl end groups were prepared via a reaction of the PEO (M_w = 2000 g/mol) with acetyl chloride in methylene dichloride. 20 g of PEO was dissolved in 200 mL of methylene dichloride with triethylamine (3 mL) and maintained in a water bath at 0 °C. During vigorous stirring, acetyl chloride was very slowly added in a stoichiometric amount, and the reaction mixture was kept at 0 °C for 3 h. Then the reaction temperature was increased to 20 °C and maintained for 24 h. The product was precipitated in dried ethyl ether and filtered. In order to eliminate insoluble impurities, the product was redissolved in hot ethanol and recrystallization. After filtering, the polymer was transferred to a vacuum oven and dried for 3 days.

The end-linked network of $PEO2_N$ and $PEO6_N$ was prepared via a reaction of the two hydroxyl end groups PEO M_w= 2000 and M_w = 6000 g/mol with 1,3,5-benzenetricarbonyl trichloride, respectively. 10 g of PEO was dissolved in 10 mL of methylene dichloride with triethylamine (1.5 mL) and maintained in a water bath at 0 °C. During magnetic stirring at the early reaction time, the solution of 1,3,5-benzenetricarbonyl trichloride (methylene dichloride as solvent) was added in stoichiometric amounts, and the reaction mixture was kept at 0 °C for 3 h. Then the reaction temperature was kept at 20 °C for 24 h. The product was dried in a vacuum oven for 1 day. In order to eliminate impurities, the product was extracted using ethanol. The blends ($PEO2_F$/$PEO2_N$ and $PEO2_F$/$PEO6_N$) of $PEO2_F$ and the end-linked network of PEOs were prepared with the same experimental procedure as that for the pure end-linked network, except the reactant is blends of the two acetyl end groups $PEO2_F$ and two hydroxyl end groups PEO with the mass ratio of 80/20. The ratio between the free chains and network is 82/18, measured through extracting the free chain after cross-link reaction, which is fairly close to the designed ratio.

Crystallization Rate Measurements. In order to obtain the samples with different strains, a homemade drawing machine was used to stretch the network. The samples were first heated from room temperature to 70 °C. After keeping the samples at

* Corresponding author. E-mail: lbli@ustc.edu.cn.

10.1021/ma802679h CCC: $40.75
Published on Web 02/17/2009

70 °C for 5 min, the samples were stretched to different strains at a deformation rate of 1.05 mm/min. Then the stretched samples maintained the strains and were cooled to the room temperature, during which the strains were frozen with solidification. For crystallization experiments, the samples with different strains were fixed on a Linkam hot stage (THM600) with a homemade clamp to maintain their initial strains. The samples were heated from room temperature to 70 °C at a rate of 10 °C/min. After held at 70 °C for 10 min, samples were cooled to the experimental temperature at a rate of 5 °C/min and held at the temperature for isothermal crystallization. The small- and wide-angle X-ray scattering (SAXS/WAXS) patterns were collected during the whole isothermal crystallization.

Simultaneous WAXS and SAXS measurements were made using an in-house setup with a sealed tube equipped with two parabolic multilayer mirrors (Bruker, Karlsruhe), giving a highly parallel beam (divergence about 0.012°) of monochromatic Cu Kα radiation ($\lambda = 0.154$ nm). The SAXS intensity was collected with a two-dimensional gas-filled wire detector (Bruker Hi-Star). A semitransparent beam stop placed in front of the area detector allowed monitoring the intensity of the direct beam. The WAXS intensity was recorded with a linear position-sensitive detector (PSD-50M, M. Braun, Germany), which could be rotated around the beam path to measure either in the meridianal or in the equatorial direction.

Results and Discussion. The isothermal crystallization behaviors of five samples—$PEO2_F$, $PEO2_N$, and $PEO6_N$ and their mixtures $PEO2_F/PEO2_N$ (82/18) and $PEO2_F/PEO6_N$ (82/18)—were studied with SAXS/WAXS at various temperatures and extension strains. Note that in the stretched mixtures stress and strain are mainly taken by the network while the short free chains suffer negligible strain. Thus, the effect of extension strain on crystallization should directly stem from the network.

We first test without EDT how the stretched network or long chain influences crystallization through the study on the $PEO2_F/PEO2_N$ (82/18) mixture. Although our focus is on the crystallization behavior of the mixtures under extension strains, the crystallization kinetics of pure $PEO2_F$ and the mixture at quiescent condition and pure $PEO2_N$ under strain were first investigated to serve as background data for comparison. $PEO2_F$ was only investigated at quiescent condition because it is difficult to impose extension. As mentioned above, in the stretched mixture, $PEO2_F$ suffers negligible strain; the referring data for comparison are the crystallization kinetics of $PEO2_F$ at quiescent condition rather than under strain. The half-time of crystallization $t_{1/2}$ was employed to represent the crystallization kinetics, and a large $t_{1/2}$ corresponds to a slow crystallization rate. $t_{1/2}$ was determined from the time evolution curve of the peak intensity from SAXS during isothermal crystallization. The WAXS data give a similar trend; thus, we only give SAXS data here.

Figure 1a gives the $t_{1/2}$ of $PEO2_F$, $PEO2_N$, and their mixtures $PEO2_F/PEO2_N$ (82/18) at different temperatures T_c and strains, respectively. Without deformation, the $t_{1/2}$ of $PEO2_F$, $PEO2_F/PEO2_N$ (82/18), and $PEO2_N$ follow a sequence of increase. Evidently cross-linking PEO short chains into a network restricts the diffusion, which decreases both nucleation and growth rates of crystal. Although imposing deformation significantly reduces the $t_{1/2}$ of $PEO2_N$, it is still much longer than that of $PEO2_F$ under zero strain. At 37 and 38 °C, crystallization of $PEO2_N$ with strains of 150% and 100% did not start after 180 min, while $PEO2_F$ at quiescent condition completed the whole crystallization process within 100 min. The slow crystallization

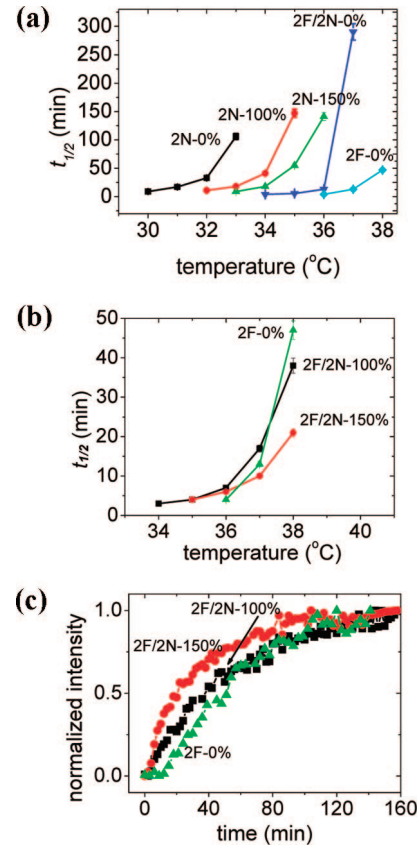

Figure 1. Plot of the half-time of crystallization $t_{1/2}$ vs temperature: (a) $PEO2_N$ under strains and $PEO2_F$ at quiescent and (b) PEO2F/PEO2N (82/18) under strains. (c) The SAXS peak intensity evolution of $PEO2_F/PEO2_N$ (82/18) during crystallization at 38 °C. The "PEO" in the sample name is omitted in the figure, and the digital following the name indicates the strains.

process of PEO2N is similar to the mixture with dense long chains of PE, which prevent the fast diffusion.[24]

With the above background data in hand, we focus on the crystallization behavior of the mixtures under different extension strains. Figure 1b gives the $t_{1/2}$ of $PEO2_F/PEO2_N$ (82/18) under strains of 100% and 150% at different temperatures. As mentioned early, in the mixture the strains are mainly sustained by the network and the free chains suffer negligible deformation. Thus, the reference data for comparison is the $t_{1/2}$ of pure network $PEO2_N$ under the same strains and those of pure short free chains $PEO2_F$ at quiescent conditions. As the crystallization of the pure network $PEO2_N$ did not start even after the completion of crystallization of $PEO2_F/PEO2_N$ (82/18) under the same strains at 37 and 38 °C, we only replotted the $t_{1/2}$ of pure $PEO2_F$ at quiescent conditions in Figure 1b for a direct comparison. At 37 °C, $PEO2_F/PEO2_N$ (82/18) under the strains of 150% and 100% crystallizes faster and slower than $PEO2_F$ does, respectively, while at 38 °C, the $t_{1/2}$ of $PEO2_F/PEO2_N$ (82/18) under both strains are shorter than that of $PEO2_F$. Detailed analysis of SAXS peak intensity during crystallization at 38 °C (Figure 1c) shows that the induction period of $PEO2_F/PEO2_N$ (82/18) under these strains are significantly shorter than that of $PEO2_F$. However, it takes nearly the same time for pure $PEO2_F$ and $PEO2_F/PEO2_N$ (82/18) mixture under the strain of 100% to complete the crystallization process. Evidently, the deformed network enhances the nucleation rather than the growth process.

Figure 2a shows a representative two-dimensional SAXS pattern of $PEO2_F/PEO2_N$ (82/18) mixture, which was crystallized under a strain of 150% at 37 °C. The stretching direction is

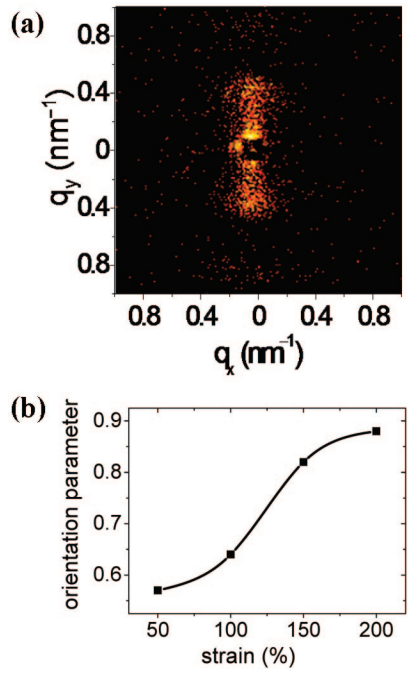

Figure 2. (a) Two-dimensional SAXS pattern of $PEO2_F/PEO2_N$ (82/18) crystallized at 37 °C under a strain of 150%. (b) Plot of orientational parameter vs the strain.

vertical. The scattering intensity is concentrated in the meridian direction, which indicates the formation of highly oriented lamellar crystals. Figure 2b gives the Herman's orientation parameter calculated from the 2D SAXS patterns of $PEO2_F/PEO2_N$ (82/18) mixtures crystallized under different strains at 37 °C. Consistent with the general observation on flow-induced crystallization of polymer, a larger strain corresponds to a larger orientation parameter of lamellar crystals.

Now we test how EDT of network or long chain influences the crystallization of the mixture through the study on the $PEO2_F/PEO6_N$ (82/18) mixture. As PEO with a molecular weight of 6000 g/mol has an equilibrium melting temperature higher than $PEO2_F$ does, under the same strain and temperature, the crystallization rates of $PEO6_N$, $PEO2_F/PEO6_N$ (82/18), and $PEO2_F$ follow a sequence of decrease.

The question we design to test is whether the partial disentangled $PEO6_N$ long segments dominate or take only a minor share in oriented nuclei in the $PEO2_F/PEO6_N$ mixture. $PEO6_N$ and $PEO2_F$ form once-folded and extended-chain crystals at the temperature range we studied, which give the first-order SAXS peaks at different q of about 0.33 and 0.45 nm^{-1}, respectively. $q = 4\pi \sin\theta/\lambda$ is the module of the scattering vector, where 2θ and λ are the scattering angle and the wavelength of X-ray, respectively. The difference of the scattering peak position allows us conveniently checking whether a phase separation occurs or $PEO6_N$ generates the nuclei alone first during the strain-induced crystallization. A relatively high crystallization temperature at 43 °C and under a strain of 200% was chosen to differentiate the nucleation barrier of the long chain $PEO6_N$ network and the short free chain $PEO2_F$. Figure 3a gives the first-order peaks from the Lorentzian corrected one-dimensional SAXS curves of $PEO2_F/PEO6_N$ (82/18) at the beginning (2F/6N-A in Figure 3a) and at the end (2F/6N-B in Figure 3a) of crystallization. For the convenience of comparison, the same scattering peaks of pure $PEO2_F$ and $PEO6_N$ are also plotted in Figure 3a. All peaks in Figure 3a are normalized for a better view and do not represent the actual

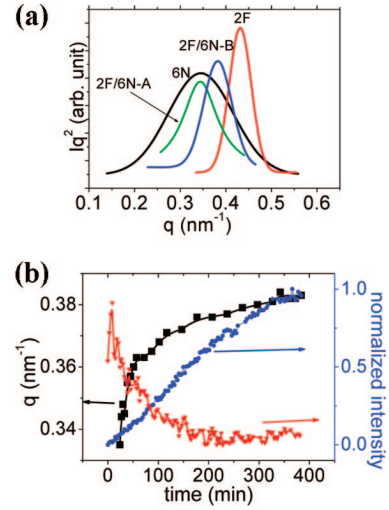

Figure 3. (a) First-order SAXS peaks of PEO2F/PEO6N (82/18) at the beginning (2F/6N-A) and the end (2F/6N-B) of crystallization under a strain of 200% at 43 °C. (b) The q value, the normalized intensity of the first-order SAXS peak, and the normalized equatorial scattering intensity during the crystallization process.

intensity. The q value and the normalized intensity of the first-order peak during the crystallization process are plotted vs crystallization time in Figure 3b. The normalized equatorial scattering intensity of SAXS near the beam stop is also plotted in Figure 3b, which is scattered from the oriented nuclei. The equatorial scattering intensity increases in the first 9 min, which decreases monotonically after reaching a maximum. The first increase of intensity is due the formation of the oriented nuclei, while the lateral growth of lamellae leads to the later decrease of intensity. At the beginning of crystallization of $PEO2_F/PEO6_N$ (82/18), the q value is nearly the same as that of pure $PEO6_N$ network, which sharply increases to a value in between the pure $PEO2_F$ and $PEO6_N$. The large long period at the beginning of crystallization should be mainly contributed by $PEO6_N$ due to lower nucleation barrier. The growth of lamellar stacks, contributed by the mixture of $PEO6_N$ and $PEO2_F$ with a shorter spacing, increases the q value, which finally reaches a q value between those of the pure $PEO6_N$ and the $PEO2_F$. We did not observe double SAXS peaks in the final crystallized sample, which is possibly due to that the initial SAXS peak at small q value is far too weak compared to the scattering from the lamellar stacks. Note the nucleation process may involve concentration fluctuation, which leads PEO6N as the main contributor, while the growth of lamellar stacks are shared by both $PEO6_N$ and $PEO2_F$, as the growth requires to overcome lower energy barrier than that for the formation of primary nuclei. The decrease of long period during crystallization process does not occur at low crystallization temperatures of this sample and at all temperatures we studied on $PEO2_F/PEO2_N$ (82/18) and $PEO6_N$. Combining the intensity evolution in at equatorial direction and the evolution of long period during crystallization at 43 °C, the stretched $PEO6_N$ network initiates the nucleation and is the main contributor of the primary oriented nuclei.

How does the stretched network promote the nucleation process in the $PEO2_F/PEO2_N$ (82/18) mixture? A possible explanation may be the strain-induced concentration fluctuation, which was illustrated by the well-known butterfly pattern of small-angle neutron scattering.[25] The strain-induced concentration fluctuation may lead to local concentration enrichment of the network and the free chains. As the pure $PEO2_N$ network under the same strain *does not* start to crystallize before the mixture completes the crystallization process at high tempera-

tures, the acceleration of nucleation is certainly not due to the local enrichment of the network. The same reasoning can also be applied to compare the stretched mixture and the pure free chains, as $PEO2_F/PEO2_N$ (82/18) mixtures under the strains nucleate faster than pure $PEO2_F$ at quiescent conditions. Thus, the strain-induced concentration fluctuation is certainly not responsible for the acceleration of nucleation. The second explanation might be the solvent effect of free chains on the stretched network, which can enhance the diffusion of network to some extent and might promote the network to form nuclei alone. However, at high temperature the rate limit factor for $PEO2_N$ to crystallize is the nucleation barrier rather than diffusion. Assuming $PEO2_F$ acts as "solvent", the diffusion factor indeed is enhanced, but the nucleation barrier is further increased due to the reduction of supercooling by "solvent". This trade-off may make $PEO2_N$ more difficult to nucleate alone. Moreover, if $PEO2_F$ only helps PEO2N to diffuse and later form the nuclei alone, PEO2N should first segregate into nanodomains as the primary nuclei should have a critical size in nanometers rather than molecular scale. After segregation, nucleation will be the same as that in the pure $PEO2_N$ network, which does not occur at all even after the mixture finished the crystallization at this temperature. Thus, in the mixture either $PEO2_N$ or $PEO2_F$ alone cannot accelerate the nucleation.

The only explanation on the acceleration of nucleation in the stretched $PEO2_F/PEO2_N$ (82/18) mixture is the synergetic effect between the orientation of $PEO2_N$ network and the fast diffusion of the short free $PEO2_F$ chains. The nucleation rate I^* can be expressed as the following equation:[26]

$$I^* = I_0 \exp\left(-\frac{E_a}{kT_c}\right) \exp\left[-\frac{\Delta G^*}{kT_c}\right] \quad (1)$$

where k and I_0 are the Boltzmann constant and a prefactor, respectively. E_a and ΔG^* are the activation energy for diffusion and the energy barrier for the formation of critical nucleus, respectively. Accounting for the effect of flow field on the nucleation in early work, ΔG^* is reduced due to conformational entropy loss, while E_a is treated as a constant.[27] As the memory function is dependent on reptation time τ_d and $\tau_d \propto M^{3.4}$, long chains always store higher orientation and have a much smaller ΔG^* than short chains do.[21] This is the essential physical origin of Keller and de Gennes' frame for flow-induced crystallization of polymer. However, the advantage of long chains or network on storing orientation exactly corresponds to a disadvantage on diffusion. Correspondingly, E_a of long chains is also much larger than that of short chains, whose effect on nucleation is well demonstrated by the slow crystallization rate of the pure network $PEO2_N$ (see Figure 1). For polymer melts at the temperatures normally employed to study flow-induced crystallization, E_a is thought to be less critical as the rate limited term is the nucleation barrier ΔG^*. However, as soon as ΔG^* is significantly dropped down by flow field, the rate limited term may switch from ΔG^* to E_a. Thus, early theory accounting only ΔG^* is certainly not sufficient to describe flow-induced crystallization of polymer. The conflict between ΔG^* and E_a is solved through blending long and short chains together, where long and short chains are responsible for storing orientation and diffusing, respectively. Note the orientation is not only stored on the network segment but also weakly imposes on the surrounding free chains.[28] Thus, the promotion on crystallization of polymer by flow field is magnified through blending long and short chains.

The molecular picture based on current experiment is in agreement with the idea from Kimata et al.[18] and Zhang et al.[19]

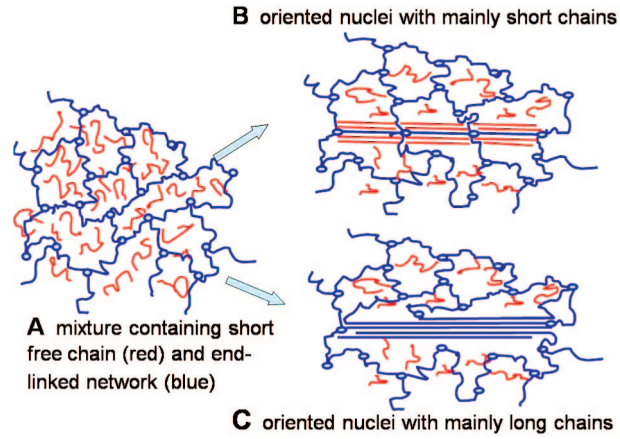

Figure 4. Nucleation model for flow-induced crystallization: (a) the oriented nuclei with mainly short chains; (b) the oriented with mainly disentangled long chains.

The former suggests that the oriented nuclei induced by flow field involving more short or medium chains instead of long chains. As discussed above, the nuclei are certainly not due to the aggregation of the segments of network or long chains. In the $PEO2_F/2_N$ (82/18) mixture one segment of the network is surrounded by about four short free chains, which are the main contributor of the oriented nuclei. Zhang et al. suggests that the formation of oriented nuclei may not involve in EDT. As the network is built with permanent "entanglement", the enhancement of nucleation by the stretched network in the $PEO2_F/PEO2_N$ (82/18) mixture provides a direct evidence on their proposal. Because every stretched segment of the network is surrounded by four free short chains, the nucleation induced by the stretched network is essentially a single chain based on nucleation, which is in consistent with the computer simulation from Hu et al.[17] Nevertheless, considering the critical size of nuclei, a collective effect from adjacent multiple single pre-aligned chains may be more efficient to initiate nucleation.

The results from the $PEO2_F/PEO6_N$ (82/18) mixture demonstrate that the long chains can be the main contributor of the oriented nuclei during flow-induced crystallization of polymer, provided that the long and the short chains have different "effective" melting temperatures. Our results are nicely in agreement with recent reports from Balzano et al.[14] and Hsiao et al.,[15] who showed that the long chains are the major component of the oriented nuclei. Both groups investigated the blends of long and short chains where the long chains have a higher "effective" melting temperature. We use "effective" melting temperature, as crystallization under flow field is a nonequilibrium thermodynamic process and the melting temperature is increased under flow. The melting temperature difference of Hsiao's material already comes from the defects in short chain, while the EDT and orientation under shear flow increases the "effective" melting temperature of long chains in Balzano et al.'s samples.

Combining the results from $PEO2_F/PEO2_N$ and $PEO2_F/PEO6_N$ mixtures, we reach a consensus picture of flow-induced crystallization of polymer, which unites the discrepancies from different facets. (i) Without EDT in the blends of minor long and major short chains, the flow-induced oriented nuclei are mainly built with the short chains (Figure 4 B). This is in agreement with the view of Kimata et al.[18] and Zhang et al.[19] (ii) With the presence of EDT, oriented nuclei are mainly made up of (partially) disentangled long chains (Figure 4 C). This is consistent with the reports from Balzano et al.[14] and Hsiao et

al.[15] From our view, the first case occurs more commonly in polymer melt during processing, while the latter one dominates in polymer solution. Here the solution is in a general sense. During flow-induced crystallization, the temperature is lower and higher than the melting temperatures of the long chain and short chain, respectively; the mixture should be treated as solution.

It is well-known that flow-induced oriented nuclei have a higher melting temperature than kebab does although oriented nuclei may not be the really extended-chain crystal. The increase of melting temperature of oriented nuclei is certainly due to the flow-induced EDT. As demonstrated by the results from $PEO2_N$ and $PEO2_F/PEO2_N$, without EDT, the lamellar crystals can only reach a maximum thickness as the full extended-chain length of mesh size or segments with a M_e. With EDT, $PEO6_N$ forms a thicker crystal with a higher melting temperature than the extended-chain length of PEO segments with the M_e, though $PEO6_N$ is still not fully extended. As EDT increases the "effective" melting temperature of crystal, the flow-induced crystallization is not only due to an entropy loss but also promoted with an enthalpy effect.[9,13] This fits well with the report on polyethylene (PE) from Balzano et al.[14] Their shish formed at temperature well above the melting temperature of kebab, where the formation of shish certainly requires EDT to provide longer unentangled segments for the formation of thicker crystals. We speculate that the increase of the "effective" melting temperature induced by EDT is more pronounced in polymers like PE and PEO with a small M_e. The M_e of PE is about 1000 g/mol, which corresponds to an extended chain length of about 9 nm.[28] Similarly, PEO has a M_e of about 2000 g/mol, corresponding to an extended chain length of 12.5 nm. Those lengths are less than the lamellar thickness of long chain PE and PEO crystallized at relative small supercooling. A direct consequence of EDT allows polymer forming a thicker crystal with a higher melting temperature. This effect may not be so significant in polymer with a large M_e like isotactic polypropylene (iPP).[29] The M_e is about 6900 g/mol for iPP, corresponding to an extended chain length of about 35 nm, which is already much larger than the lamellar thickness formed at normal condition for the study of flow-induced crystallization. Without disentanglement, the oriented iPP network with the mesh size of the M_e can already form a much thicker crystal with a higher melting temperature than crystal obtained at quiescent conditions.

An additional role of EDT is on the diffusion. It is well-known that EDT leads to a reduction of viscosity or the so-called shear thinning, which means the diffusion of chains after EDT is much faster than chains without EDT. Thus, EDT promotes nucleation not only on reduction of the nucleation barrier but also on enhancement of chain diffusion.

Conclusion. In summary, the nature of hierarchical crystallization of polymer under flow field was studied on two simplified mixtures of short free chains and end-linked network, which were designed to mimic the blend of short and long chains. With a mesh size as the same as the M_e, where no disentanglement occurs, the acceleration of nucleation in the stretched mixtures stem from the synergetic effect between the orientation of the network and the fast diffusion of the free chains, which renders the oriented nuclei composing mainly of short free chains. With the occurrence of EDT in the network with large mesh size, the long chains are the main contributor of the oriented nuclei, in agreement with the traditional view. The former may be the general case in polymer melt, while the latter occurs mainly in polymer solution. Correspondingly, the "row nuclei" for melt and "shish" for solution should be restricted to their initial definition and not be interchangeable, as molecular pictures of them are indeed different.

Acknowledgment. The authors thank Prof. Julia Kornfield (Caltech), Prof. Shiqing Wang (Akron), and Prof. Wenbing Hu (Nanjing) for their valuable discussion and suggestion on this work. L. Li thanks Prof. Wim de Jeu for great help to build the soft matter group in Hefei. This work is supported by the National Natural Science Foundation of China (50503015, 20774091), one hundred talent scientist program, and the "NCET" program of the Minister of Education. The research is also in part supported by the Opening Project of the State Key Laboratory of Polymer Materials Engineering (Sichuan University).

References and Notes

(1) Bashir, Z.; Odell, J. A.; Keller, A. *J. Mater. Sci.* **1986**, *21*, 3993–4002.
(2) Pennings, A. J.; Kiel, A. M.; Kolloid, Z. Z. *Polymer* **1965**, *205*, 160–162.
(3) Binsbergen, F. L. *Nature (London)* **1966**, *211*, 516–517.
(4) Azzurri, F.; Alfonso, G. C. *Macromolecules* **2005**, *38*, 1723–1728.
(5) Somani, R. H.; Yang, L.; Hsiao, B. S. *Polymer* **2005**, *46*, 8587–8623.
(6) Li, L. B.; De Jeu, W. H. *Adv. Polym. Sci.* **2005**, *181*, 75–120.
(7) Somani, R. H.; Hsiao, B. S.; Nogales, A.; Srinivas, S.; Tsou, A. H.; Sics, I.; Balta-Calleja, F. J.; Ezquerra, T. A. *Macromolecules* **2000**, *33*, 9385–9394.
(8) Kume, T.; Hattori, T.; Hashimoto, T. *Macromolecules* **1997**, *30*, 427–434.
(9) Kanaya, T.; Matsuba, G.; Ogino, Y.; et al. *Macromolecules* **2007**, *40*, 3650–3654.
(10) Balzano, L.; Rastogi, S.; Peters, G. W. M. *Macromolecules* **2008**, *41*, 399–408.
(11) Keller, A.; Kolnaar, H. W. H. *Flow Induced Orientation and Structure Formation*; VCH: New York, 1997; Vol. 18.
(12) de Gennes, P. G. *J. Chem. Phys.* **1974**, *60*, 5030–5042.
(13) Seki, M.; et al. *Macromolecules* **2002**, *35*, 2583–2594.
(14) Balzano, L.; et al. *Phys. Rev. Lett.* **2008**, *100*, 048302.
(15) Hsiao, B. S.; et al. *Phys. Rev. Lett.* **2005**, *94*, 117802.
(16) Dukovski, I.; Muthukumar, M. *J. Chem. Phys.* **2003**, *118*, 6648–6655.
(17) Hu, W.; Frenkel, D.; Mathot, V. B. F. *Macromolecules* **2002**, *35*, 7172–7174.
(18) Kimata, S.; et al. *Science* **2007**, *316*, 1014–1017.
(19) Zhang, C.; et al. *Polymer* **2005**, *46*, 8157–8161.
(20) Wang, S. Q.; Ranvindranath, S.; Boukany, P.; Olechnowicz, M.; Quirk, R. P.; Halasa, A.; Mays, J. *Phys. Rev. Lett.* **2006**, *97*, 187801.
(21) Doi, M.; Edwards, S. F. *The Theory of Polymer Dynamics*; Clarendon Press: Oxford, UK, 1986.
(22) Hild, G. *Prog. Polym. Sci.* **1998**, *23*, 1019–1149.
(23) Fetters, L. J.; Lohse, D. J.; Milner, S. T.; Graessley, W. W. *Macromolecules* **1999**, *32*, 6847–6851.
(24) Ogino, Y.; Fukushima, H.; Matsuba, G.; Takahashi, N.; Nishida, K.; Kanaya, T. *Polymer* **2006**, *47*, 5669.
(25) Mendes, E.; Lindner, P.; Buzier, M.; Bod, F.; Bastide, J. *Phys. Rev. Lett.* **1991**, *66*, 1595–1598.
(26) Wunderlich, B. *Macromolecular Physics*; Academic Press: New York, 1976; Vol. 2.
(27) Coppola, S.; Grizzuti, N.; Maffettone, P. L. *Macromolecules* **2001**, *34*, 5030–5036.
(28) Deloche, B.; Dubault, A.; Herz, J.; Lapp, A. *Europhys. Lett.* **1986**, *1*, 629–635.
(29) Fetters, L. J.; et al. *Macromolecules* **2002**, *35*, 10096–10101.

MA802679H